Chain-Length Dependence of Insertion, Desorption, and Translocation of a Homologous Series of 7-Nitrobenz-2-oxa-1,3-diazol-4-yl-Labeled Aliphatic Amines in Membranes

ARTICLE *in* THE JOURNAL OF PHYSICAL CHEMISTRY B · AUGUST 2011

Impact Factor: 3.3 · DOI: 10.1021/jp203429s · Source: PubMed

6 AUTHORS, INCLUDING:

Patrícia Martins
King Abdullah University of Science and Tec…
8 PUBLICATIONS **31** CITATIONS
SEE PROFILE

Filipe Gomes
University of Coimbra
13 PUBLICATIONS **111** CITATIONS
SEE PROFILE

Slavomira Doktorovova
25 PUBLICATIONS **281** CITATIONS
SEE PROFILE

Maria João Moreno
University of Coimbra
47 PUBLICATIONS **546** CITATIONS
SEE PROFILE

THE JOURNAL OF PHYSICAL CHEMISTRY B

ARTICLE

pubs.acs.org/JPCB

Chain-Length Dependence of Insertion, Desorption, and Translocation of a Homologous Series of 7-Nitrobenz-2-oxa-1, 3-diazol-4-yl-Labeled Aliphatic Amines in Membranes

Renato M. S. Cardoso, Patricia A. T. Martins, Filipe Gomes, Slavomira Doktorovova, Winchil L. C. Vaz, and Maria João Moreno*

Departamento de Química, Faculdade de Ciencias e Tecnologia da Universidade de Coimbra (FCTUC), Largo D. Dinis, Rua Larga, 3004-535 Coimbra, Portugal

ABSTRACT: We present a complete characterization of the kinetics of interaction between the homologous series of fluorescent fatty amines with the fluorescent moiety 7-nitrobenz-2-oxa-1,3-diazol-4-yl covalently bound to the amine group, NBD-C_n ($n = 8-16$), and a lipid bilayer in the liquid disordered phase. The insertion into and the desorption from the lipid bilayer, as well as the rate of translocation across the two bilayer leaflets, has been measured at different temperatures, allowing an estimation of the thermodynamic parameters in the formation of the transition state. This is the first report on the complete characterization of the kinetics of the interaction of a large series of structurally homologous amphiphiles. In a recent paper from this research group, the equilibrium interaction of NBD-C_n ($n = 4-10$) with POPC bilayers and serum albumin was reported. This information allows the calculation of the equilibrium distribution of the amphiphiles among the aqueous phase, serum proteins, and biomembranes. The data presented in this manuscript complement its characterization with information on the kinetics of the interactions, making possible the quantitative evaluation of their pharmacokinetics. The rate of translocation is shown to decrease with increasing alkyl chain length up to $n = 12$, becoming relatively insensitive to further increases in n. The Gibbs free energy variation associated with the rate of desorption from the lipid bilayer increased linearly with n, with $\Delta\Delta G^{\ddagger o} = 3.4 \pm 0.5$ kJ mol^{-1} per methylene group. It was also found that the process of insertion in the lipid bilayer is not diffusion-limited, although it is close to this limit for the smaller amphiphiles in the homologous series at high temperatures.

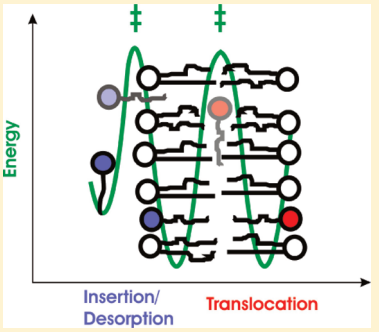

INTRODUCTION

The bioavailability of amphiphilic molecules is strongly determined by their interaction with proteins and lipid assemblies in the blood and inside cells. To a first approximation the equilibrium interaction with the different binding agents may be considered allowing the calculation of the ligand fraction in each environment at equilibrium. However, for the accurate characterization of its pharmacokinetics and bioavailability, the rate constants for the different steps in the interaction of the ligand with the biological system must be known. We have recently reported on the equilibrium parameters of the 7-nitrobenz-2-oxa-1,3-diazol-4-yl (NBD)-C_n homologous series in aqueous solution and its binding to 2-oleoyl-1-pamlitoyl-*sn*-glycero-3-phosphocholine (POPC) lipid bilayers and bovine serum albumin (BSA).[1] In this work we have experimentally measured the rate constants for the interaction of the amphiphiles in this homologous series with lipid bilayers (insertion/desorption and translocation) and give a lower limit for the rate of their interaction with BSA. This information may be used for the accurate calculation of the rate of passive permeation of those amphiphiles through lipid membranes and may be used to predict the permeation through cell monolayers, representing a step forward in the quantitative description of amphiphile pharmacokinetics.

This work represents the first homologous series where all the rate constants for the interaction with lipid bilayers are quantitatively characterized in a single or in multiple studies. As a comparison, in the case of the extensively studied homologous series of saturated and unsaturated fatty acids, hundreds of publications may be found in the literature, but only the rate of desorption has been accurately measured.[2−4]

For some amphiphiles two out of the three rate constants required for the full characterization of their interaction with lipid bilayers (insertion, desorption, and translocation) have been measured.[5−9] However, those studies cannot be used to calculate the pharmacokinetics of the amphiphiles due to the inexistence of the third parameter. An exception is the characterization by this group of the interaction of NBD-1,2-dimyristoyl-*sn*-glycero-3-phosphoethanolamine (DMPE) and NBD-lysomyristoylphosphatidylethanolamine (LysoMPE) with membranes of different lipid composition.[10−12] Those two amphiphiles may be considered a homologous series where the property changing among the series is the number of acyl chains, and the comparison between the

Received: April 12, 2011
Revised: July 6, 2011
Published: July 12, 2011

dx.doi.org/10.1021/jp203429s | *J. Phys. Chem. B* 2011, 115, 10098–10108

results has led to important conclusions, namely: (i) The number of acyl chains does not significantly influence the rate of translocation.[10] (ii) The insertion in the lipid bilayer is not diffusion-controlled, being dependent on the cross section of the hydrophobic portion of the amphiphile,[11−13] and (iii) the rate of desorption is dependent on the hydrophobicity of the amphiphile. However, the small size of this series does not allow quantitative conclusions and is not enough for the interpretation of the contribution from the different chemical groups on the amphiphiles.

The methodology followed in this work is also a significant advancement relative to previous studies, namely, (i) the use of very small concentrations of amphiphiles to minimize perturbation of the bilayer, (ii) previous calculation of their solubility to guarantee that there was no amphiphile aggregation in the aqueous phase, (iii) use of two independent methods, one being more sensitive to translocation and the other to the association with the lipid bilayer, and (iv) characterization of the interaction with the lipid bilayer at different concentrations of acceptor. In previous publications by other authors both the association and the translocation processes are tentatively obtained from a single transfer experiment, usually with a single acceptor concentration, and in some cases no special care is given to amphiphile aggregation. That approach is extremely prone to artifacts, specially coming from amphiphile aggregation and/or probe photobleaching, and has led to conflicting results by different research groups being one of the origins of data-scatter and lack of consensus on the interaction of fatty acids with lipid bilayers.

With the full characterization of the different steps in the interaction between the amphiphiles and the lipid bilayers, it is possible to calculate the rate of passive permeation through membranes or cell monolayers. The use of homologous series allows the establishment of relations between the structural properties of the amphiphile and the value of the observed parameter leading to the development of rules with predictive value. The currently accepted model for passive permeation across lipid bilayers assumes fast equilibration of amphiphile between the aqueous and the membrane phases and slow diffusion (translocation) through the lipid bilayer.[14] Within this model the partition coefficient between the aqueous and the membrane phases and the translocation rate constants are the important parameters in the prediction of the rate of passive permeation. Surprisingly, the actual predictors for the rate of passive permeation of a given amphiphile are based mostly on their hydrophobicity, with the rate of translocation (assumed to be the rate-limiting step) being usually unknown and not explicitly considered.[15] Not surprisingly, therefore, recent studies have shown the breakdown of this simple model for very hydrophobic ligands.[16,17] To understand the limitations of the model and to be able to build a more appropriate one, it is necessary to quantitatively characterize the kinetics of the interaction of the ligands with the lipid bilayer as well as their rate of translocation across it for several structurally related molecules (a homologous series). The characterization of the NBD-C_n homologous series presented in this work is an important step in that direction.

MATERIALS AND METHODS

Materials. POPC was from Avanti Polar Lipids, Inc. (Alabaster, Alabama, GA, USA), and BSA was from Applichem (Darmstadt, Germany). All other reagents and solvents were of analytical grade, or higher purity, from Sigma-Aldrich Química S.A. (Sintra, Portugal).

Equipment. Steady state fluorescence measurements were performed on a Cary Eclipse fluorescence spectrophotometer (Varian) equipped with a thermostatted multicell holder. UV−vis absorption was performed on a Unicam UV530 spectrophotometer (Cambridge, UK). Stopped-flow measurements were performed as previously described[18] on a thermostatted stopped-flow fluorimeter (Hi-Tech model SF-61). Data were analyzed using Microsoft Excel and Solver.

Rate of Translocation of NBD-C_n through POPC Bilayers. The kinetics of translocation of the amphiphiles was followed via the irreversible quenching of NBD by dithionite added to the aqueous solution outside the lipid vesicles.[10,19] The quenching of NBD was biphasic with a fast decrease in the fluorescence to about half the initial value due to reaction of dithionite with NBD-C_n in the outer monolayer followed by slower fluorescence depletion due to reaction with NBD that was initially in the inner monolayer. The permeation of dithionite through the bilayer was negligible during the time required for complete quenching of NBD,[10] and therefore, the slow process was due to the translocation of NBD-C_n from the inner to the outer leaflet of POPC bilayers. This method could not be used for the case of NBD-C_8 because the rate of translocation was not slower then the reaction of dithionite with NBD in the outer monolayer, and therefore a monoexponential fluorescence decrease was observed. For this amphiphile, the rate of translocation was obtained from the global fit of its interaction with POPC vesicles for different lipid concentrations.

Rate of Interaction of NBD-C_n with POPC Bilayers. For amphiphiles with a solubility in the aqueous medium higher than 10 nM (NBD-C_8 and NBD-C_{10}[1]), the kinetics of its interaction with POPC bilayers was studied directly via the addition of POPC to an aqueous solution (4-(2-hydroxyethyl)-1-piperazineethanesulfonic acid (HEPES) 10 mM at pH = 7.4 with 0.15 M NaCl, 1 mM ethylenediaminetetraacetic acid (EDTA), and 0.02% NaN_3) of the amphiphile. The aqueous solutions of the amphiphile were freshly prepared before each experiment by squirting a small aliquot of a solution of amphiphile in methanol while stirring gently with a vortex apparatus. The final methanol concentration was always 0.5%. This solution was then mixed (using the stopped-flow equipment) with an equal volume of solutions of POPC in the same buffer, and the increase in NBD fluorescence due to binding to the POPC bilayer followed. The direct interaction of the amphiphiles with longer alkyl chains (NBD-C_{12} to NBD-C_{16}) with the POPC bilayer could not be followed in this manner due to their negligible solubility in the aqueous phase. They were, therefore, first bound to BSA and their transfer from BSA to POPC vesicles was followed instead. The concentration of BSA in the donor solution was such that the aqueous concentration of NBD-C_n was smaller than its CAC using the binding constants and aggregation concentrations previously reported.[1] If the binding constant to BSA was not known, the value used in the calculations was that obtained for the most similar amphiphile in this homologous series. The amphiphile was allowed to equilibrate with BSA for 1 h; this solution was mixed with POPC bilayers, and the transfer was followed by the increase in NBD fluorescence.[12] Equal volumes of the two solutions were mixed in the stopped flow apparatus for the case of NBD-C_{12} and NBD-C_{14} (in those cases transfer occurs in less than 30 min), and the transfer of NBD-C_{16} was followed in a conventional fluorescence spectrophotometer.

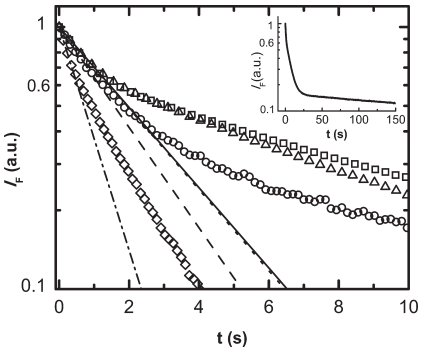

Figure 1. Quenching of NBD-C_n fluorescence, in symmetrically labeled POPC LUVs, due to the addition of dithionite to the aqueous media outside the vesicles at 25 °C, for NBD-C_{16} (□, solid line), NBD-C_{14} (○, dashed line), NBD-C_{12} (△, dotted line), and NBD-C_{10} (◇, dot−dashed line) for a concentration of dithionite equal to 20 mM for NBD-C_{12} to NBD-C_{16} and 80 mM for NBD-C_{10}. The lines represent the initial rate observed. Insert: Complete curve obtained for the fluorescence quenching of NBD-C_{16} by dithionite.

The concentration of BSA was calculated from its absorption at 279 nm using $\varepsilon = 4.4 \times 10^4\ M^{-1}\ cm^{-1}$.[20]

The POPC was in the form of large unilamellar vesicles (LUVs) that were prepared by evaporation of a POPC solution in the azeotropic mixture of chloroform and methanol (87:13, v/v) followed by hydration of the film with the aqueous buffer and subsequent extrusion (extruder from Lipex Biomembranes, Vancouver, British Columbia, Canada) through 100 nm pore size filters (Nucleopore, Whatman, Springfield Hill, U.K.). The final concentration of POPC was verified using a modified version of the Bartlett phosphate assay.[21]

The ratio of POPC to bound amphiphile was always equal or higher than 100 to guarantee that the properties of the bilayer were not affected by the ligand,[22] and the molar ratio of amphiphile to BSA was always much smaller than 1 (typically less than 1%); therefore, only binding to the highest affinity binding site on BSA needed to be considered.

RESULTS AND DISCUSSION

Rate of Translocation through the POPC Bilayer. The kinetics of translocation from the inner to the outer leaflet of the POPC bilayer was measured via the irreversible quenching of NBD by dithionite. The time dependence of NBD fluorescence after the addition of dithionite to POPC LUVs symmetrically labeled with NBD-C_n is shown in Figure 1.

A biphasic behavior is clearly seen for the case of NBD-C_{16} to NBD-C_{12}, and the fast process accounts for 40−45% of the total NBD fluorescence. For NBD-C_{10} the shift between the two regimes is not so evident, but the rate of the two processes, the reaction between dithionite and NBD initially in the outer monolayer and with NBD initially in the inner monolayer, may still be obtained although a higher concentration of dithionite had to be used (the buffer capacity was increased by using 100 mM HEPES to guarantee that the pH did not change upon addition of dithionite). For the amphiphile with the shortest alkyl chain studied in this work, NBD-C_8, the reaction of dithionite with NBD was a monoexponential for dithionite concentrations up to 160 mM, indicating that translocation was not the rate-limiting step for the reaction between dithionite and NBD initially in the inner monolayer (results not shown). This result leads to a lower limit for the rate of translocation of NBD-C_8 across POPC bilayers, $k_f \geq 1.0\ s^{-1}$ at 25 °C.

The insert of Figure 1 shows the complete time dependence of NBD-C_{16} fluorescence, and an additional process can be observed, which is significant for $t > 20$ s. This and the fact that the fast process does not account for 50% quenching of the NBD fluorescence allowed us to conclude that the LUVs contained some degree of multilamellarity (10−20% of the lipid). For those amphiphiles where the rate of translocation is much faster then the rate of desorption (case of NBD-C_{16}), the quenching of NBD initially in the inner bilayer is a much slower process, and the three processes (reaction of dithionite with NBD initially in the outer monolayer of the outer bilayer, in the inner monolayer of the outer bilayer, and in the inner bilayer) may be observed. As the alkyl chain of the amphiphile is decreased, the rate of desorption is expected to increase ≈3 times per CH_2,[3,4] and the desorption and translocation processes start overlapping in time. In this case multilamellarity leads to a decrease in the apparent rate of translocation, and it must be considered for the quantitative analysis of the results.

The complete kinetic scheme and the resulting set of differential equations describing the rate of dithionite reaction with LUVs symmetrically labeled with NBD is given by Scheme 1 and eq 1:

In this scheme, the subscripts $l_{o,o}$ and $l_{o,i}$ represent the lipid pool in the outer and inner monolayer of the outer bilayer and $l_{i,o}$ and $l_{i,i}$ represent the lipid pool in the outer and inner monolayer of the inner bilayer. NBD in the aqueous phase outside the liposomes (NBD_{wo}) or inserted in the outer leaflet of the outer bilayer of the LUVs ($NBD_{lo,o}$) is irreversibly quenched by dithionite in the aqueous phase outside the LUVs (T_o). The NBD initially inserted in the inner monolayer of the outer bilayer ($NBD_{lo,i}$) must translocate into the outer monolayer before being quenched by dithionite. In the case that the lipid vesicles are multilamellar, the NBD initially inserted in the outer or inner leaflet of the internal bilayer ($NBD_{li,o}$ or $_{NBD_i}$i,i, respectively) must additionally desorb from this internal bilayer into the aqueous phase between the two bilayers (NBD_{wi}) and insert into the outer bilayer.

$$\frac{d[\mathrm{NBD}_{wo}]_{V_T}}{dt} = -(k_R^w[T_o]_{V_o} + k_{in}S_{lo,o})[\mathrm{NBD}_{wo}]_{V_T} + k_-[\mathrm{NBD}_{lo,o}]_{V_T}$$

$$\frac{d[\mathrm{NBD}_{lo,o}]_{V_T}}{dt} = -(k_R^l[T_o]_{V_o} + k_-)[\mathrm{NBD}_{lo,o}]_{V_T} + k_{in}S_{lo,o}[\mathrm{NBD}_{wo}]_{V_T} - k_f\{[\mathrm{NBD}_{lo,o}]_{V_T} - [\mathrm{NBD}_{lo,i}]_{V_T}\}$$

$$\frac{d[\mathrm{NBD}_{lo,i}]_{V_T}}{dt} = -k_f\{[\mathrm{NBD}_{lo,i}]_{V_T} - [\mathrm{NBD}_{lo,o}]_{V_T}\} + k_{in}S_{lo,i}[\mathrm{NBD}_{wi}]_{V_i} - k_-[\mathrm{NBD}_{lo,i}]_{V_T}$$

$$\frac{d[\mathrm{NBD}_{wi}]_{V_i}}{dt} = \{-k_{in}[\mathrm{NBD}_{wi}]_{V_i}(S_{lo,i} + S_{li,o}) + k_-([\mathrm{NBD}_{lo,i}]_{V_T} + [\mathrm{NBD}_{li,o}]_{V_T})\}\frac{V_T}{V_i}$$

$$\frac{d[\mathrm{NBD}_{li,o}]_{V_T}}{dt} = -k_-[\mathrm{NBD}_{li,o}]_{V_T} + k_{in}S_{li,o}[\mathrm{NBD}_{wi}]_{V_i} - k_f\{[\mathrm{NBD}_{li,o}]_{V_T} - [\mathrm{NBD}_{li,i}]_{V_T}\}$$

$$\frac{d[\mathrm{NBD}_{li,i}]_{V_T}}{dt} = -k_f\{[\mathrm{NBD}_{li,i}]_{V_T} - [\mathrm{NBD}_{li,o}]_{V_T}\}$$

$$\frac{d[T_o]_{V_T}}{dt} = -(k_R^w[\mathrm{NBD}_{wo}]_{V_T} + k_R^l[\mathrm{NBD}_{lo,o}]_{V_T})[T_o]_{V_o} \qquad (1)$$

Scheme 1. Kinetic Steps Involved in the Reaction of Dithionite with Symmetrically Labeled LUVs with Two Bilayers per Vesicle

$$\mathrm{NBD_{wo}} \underset{k_-}{\overset{k_{in}S_{\ell o,o}}{\rightleftharpoons}} \mathrm{NBD_{\ell o,o}} \overset{k_f}{\longleftrightarrow} \mathrm{NBD_{\ell o,i}} \underset{k_{in}S_{\ell o,i}}{\overset{k_-}{\rightleftharpoons}} \mathrm{NBD_{wi}} \underset{k_-}{\overset{k_{in}S_{\ell i,o}}{\rightleftharpoons}} \mathrm{NBD_{\ell i,o}} \overset{k_f}{\longleftrightarrow} \mathrm{NBD_{\ell i,i}}$$

$$\downarrow k_R^w[\mathrm{T_o}]_{V_o} \qquad \downarrow k_R^\ell[\mathrm{T_o}]_{V_o}$$

non fluorescent product

The rate of insertion into the lipid bilayer was considered to be proportional to the lipid surface, per unit volume of the total solution, accessible to the amphiphile (S_l) with the rate constant k_{in}. This is valid in the absence of concentration gradients and should apply if the rate of insertion is not diffusion-limited as was the case for the insertion of other amphiphiles with POPC bilayers.[11−13] The surface area, per unit volume of the total solution, of each lipid pool was calculated from the corresponding lipid concentration assuming an area of 63 Å^2 per POPC molecule.[23] The amount of lipid in the outer and inner monolayer of each bilayer is considered the same, and the fraction of lipid in the inner bilayer is an adjustable parameter recovered from the best fit.

The best fit of the above set of equations to typical results obtained for NBD-C_{16} and NBD-C_{12} at 25 °C is shown in Figure 2. The concentration of amphiphile in the different compartments is also shown. The results obtained for NBD-C_{16} show that the quenching of NBD in the outer bilayer is essentially complete before the NBD initially in the inner bilayer reaches the outer one and is able to react with dithionite. The good temporal separation between the two processes allows the accurate recovery of the translocation rate constant without consideration of this complicated kinetic scheme. However, for NBD-C_{12} the two processes occur in similar time scales, and this treatment is required to obtain the translocation rate constant. Additionally, the quality of the best fit improves significantly (over 10 times) with the inclusion of liposome multilamellarity in the model.

Using the methodology discussed above, the rate constants for translocation of NBD-C_n through the POPC bilayer were obtained for C_{16} to C_{10} between 15 and 35 °C, and the thermodynamic parameters were obtained using the absolute rate theory[24−26] as done before for similar systems.[27] The results are shown in Figure 3. For the amphiphile with the shortest alkyl chain studied in this work, NBD-C_8, this experimental methodology could not be used because translocation was not the rate-limiting step. The results presented in Figure 3 were obtained from the kinetics of interaction of this amphiphile with POPC LUVs (see next section).

The first observation from the results obtained is the decrease in the rate of translocation with an increase in the length of the alkyl chain except for NBD-C_{14} where translocation was faster than observed for NBD-C_{12}. Another striking observation is that the temperature dependence of the translocation rate for NBD-C_{14} was smaller than for C_{12} or C_{16}, resulting in a significantly smaller value of the enthalpy variation associated with the formation of the transition state. This nonmonotonic behavior of the NBD-C_n series at NBD-C_{14} was also observed in the photophysical properties of the NBD group[1] and should reflect a different location of the amphiphile polar headgroup at the POPC bilayer. The plot of the Gibbs free energy variation, at 25 °C, along the homologous series (Figure 3B) clearly shows that the size of the nonpolar portion of the amphiphile

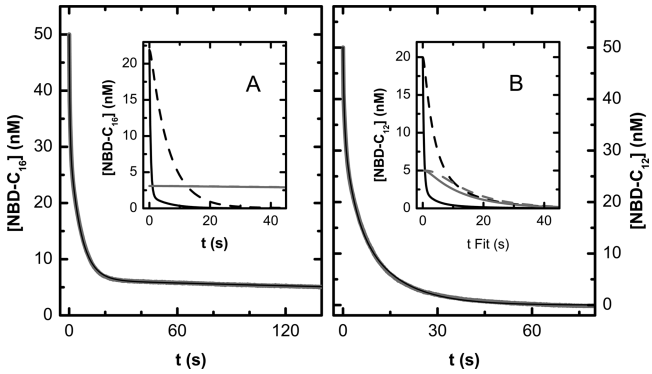

Figure 2. Quenching of NBD-C_n fluorescence, in symmetrically labeled POPC LUVs, due to the addition of 20 mM dithionite to the aqueous medium outside the vesicles, for NBD-C_{16} (gray solid line, A), and NBD-C_{12} (gray solid line, B). The line is the best fit of eq 1 to the experimental data with $k_{R_i} = k_R^w = 1.1 \times 10^2$ M^{-1} s^{-1}, $k_{in} = 1.8 \times 10^{-3}$ dm s^{-1}, $k_- = 3.4 \times 10^{-3}$ s^{-1}, $k_f = 1.8 \times 10^{-1}$ s^{-1}, and 12% of the lipid in the inner bilayer, for NBD-C_{16}; and $k_{in} = 1.1 \times 10^{-2}$ dm s^{-1}, $k_- = 3.3 \times 10^{-1}$ s^{-1}, $k_f = 2.8 \times 10^{-1}$ s^{-1}, and 20% of the lipid in the inner bilayer for NBD-C_{12}. The insert shows the time evolution of the concentration of NBD in the different compartments of the lipid bilayer: $NBD_{lo,o}$ (black solid line), $NBD_{lo,i}$ (black dashed line), $NBD_{li,o}$ (gray solid line), and $NBD_{li,i}$ (gray dashed line). The insertion rate constant considered was obtained from a preliminary analysis of the results obtained for the association of NBD-C_n with POPC LUVs; the other parameters were obtained from the best fit.

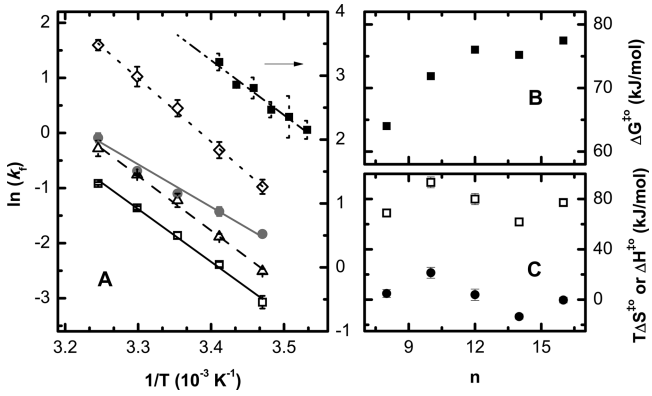

Figure 3. Kinetics and thermodynamics of translocation of NBD-C_n through POPC bilayers. (A) Experimental results obtained for NBD-C_{16} (□, solid line), NBD-C_{14} (gray ●, solid line), NBD-C_{12} (△, dashed line), NBD-C_{10} (◇, dotted line), and NBD-C_8 (■, dot−dashed line). The lines are the best fit of the absolute rate theory with the thermodynamic parameters at 25 °C shown in B for $\Delta G^{‡o}$ (■) and C for $\Delta H^{‡o}$ (□) and $T\Delta S^{‡o}$ (●). The results for NBD-C_{10} to C_{16} were obtained from the rate of quenching by dithionite, and those for NBD-C_8 were obtained from the rate of interaction with POPC LUVs. The values shown are the average and standard deviation of at least three independent experiments.

influences strongly its rate of translocation for alkyl chains up to 12 carbons ($\Delta\Delta G^{‡0} = 3.9$ kJ mol^{-1} from C_8 to C_{10} and 2.1 kJ mol^{-1} from C_{10} to C_{12}) being less sensitive for longer alkyl chains. The comparison of our results with literature values is difficult as there are very few studies on the effect of amphiphile hydrophobicity on the rate of translocation through lipid bilayers. An exception is the translocation of phosphatidylcholines with pyrene in the *sn*2 chain and different lengths of the

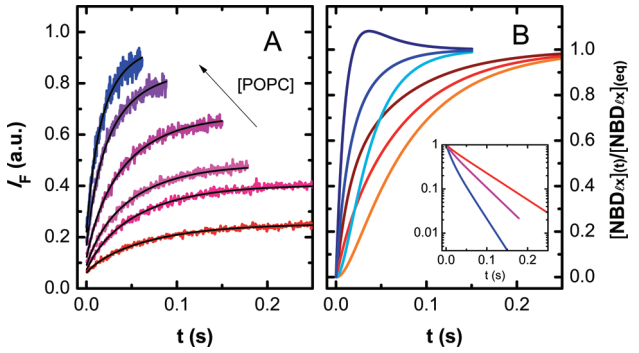

Figure 4. Rate of association of NBD-C_8 with POPC LUVs at 20 °C. (A) Experimental results obtained for LUVs with [LUV] equal to 0.54 (orange line), 1.1 (red line), 1.6 (pink line), 2.2 (magenta line), 4.3 (purple line), and 6.5×10^{-10} M (blue line). The black lines are the global best fits of eq 2 with the rate constants $k_+ = 6.8 \times 10^{10}$ M^{-1} s^{-1}, $k_- = 3.2 \times 10^{1}$ s^{-1}, and $k_f = 2.6 \times 10^{1}$ s^{-1}. (B) Simulation of the concentrations of NBD-C_8 in the different compartments, with the same rate constants as in A, for [LUV] = 0.54×10^{-10} M (NBD_{lo} + NBD_{li}, red line; NBD_{lo}, brown line; NBD_{li}, orange line) and [LUV] = 6.5×10^{-10} M (NBD_{lo} + NBD_{li}, blue line; NBD_{lo}, navy line; NBD_{li}, light blue line). The insert shows the normalized deviation of the total concentration of amphiphile in the bilayer from its equilibrium concentration, for [LUV] equal to 0.54 (red line), 2.2 (magenta line), and 6.5×10^{-10} M (blue line), to highlight the deviations from a monoexponential profile.

acyl group in the *sn*1 position (8−12 carbons)[9] where a decrease in the rate of translocation with the increase in the acyl chain length was observed ($\Delta\Delta G^{\ddagger 0}$ = 0.89 kJ mol^{-1}). Figure 3C shows the enthalpic and entropic contributions to the Gibbs free energy for the translocation process. The first observation is the enthalpy/entropy compensation that leads to little variation in the Gibbs free energy along the series despite the strong variation in enthalpy and entropy. Another observation is that the enthalpy variation upon the formation of the transition state in the translocation of NBD-C_{14} is the smallest along the series (as was already evident in the plot of the translocation rate versus $1/T$ (Figure 3A) with significantly smaller temperature dependence) which is compensated by the smallest increase in entropy. The enthalpy contribution is largest for NBD-C_{10} being compensated by a large increase in entropy when going from the inserted to the translocation transition state.

The variation observed in the thermodynamic parameters upon the formation of the transition state is expected to depend strongly on the interactions between the polar NBD group and the lipids/water at the bilayer interface when the amphiphile is inserted in the bilayer. The results obtained may reflect differences in the position of the NBD group relative to the bilayer interface with larger or smaller interactions with the lipid polar groups and water. Within the context of this interpretation it is tempting to speculate that NBD-C_{10} is more exposed to the solvent while NBD-C_{14} is deeper in the lipid bilayer with NBD-C_{12} representing the transition between short and long alkyl amphiphiles. Our results obtained using molecular dynamics simulations of the different NBD-C_n inserted in POPC bilayers support this interpretation.[28]

Rate of Interaction with the POPC Bilayer, Insertion, and Desorption. The interaction of the amphiphiles with POPC was followed via the increase in NBD fluorescence when inserted in the lipid bilayer. For the shorter alkyl chain amphiphiles (NBD-C_8 and NBD-C_{10}) the transfer from the aqueous solution to the lipid bilayer was followed directly, but this approach could not be used for the other amphiphiles due to their low solubility in the aqueous medium.[1] For NBD-C_{12} to NBD-C_{16}, the interaction with the POPC bilayer was therefore studied following the transfer of the amphiphile from BSA to POPC LUVs which occurs via the monomer in the aqueous medium.[12,18] The results obtained at 25 °C are presented in Figures 4 to 6 and Table 1.

The kinetic scheme describing the transfer of NBD-C_n from BSA to the POPC bilayers is given by Scheme 2, and the corresponding set of differential equations for the time evolution of the amphiphile in the different compartments is given by eq 2.

The association of NBD-C_n with BSA is assumed to be in fast equilibrium. This approximation is validated by the linear dependence of the characteristic rate constant for transfer with the concentration of LUVs, as in Figure 6B. When the dissociation from the donor is the rate-limiting step in the amphiphile transfer, the dependence of the overall rate on the concentration of acceptor shows a downward curvature approaching the rate constant for desorption from the donor at high concentrations of acceptor.[5,29]

$$\frac{d[\mathrm{NBD}_{lo}]}{dt} = k_+[\mathrm{NBD}_w] - k_-[\mathrm{NBD}_{lo}] - k_f([\mathrm{NBD}_{lo}] - [\mathrm{NBD}_{li}])$$

$$\frac{d[\mathrm{NBD}_{li}]}{dt} = -k_f([\mathrm{NBD}_{li}] - [\mathrm{NBD}_{lo}])$$

$$\frac{d[\mathrm{NBD}_l]}{dt} = \frac{d[\mathrm{NBD}_{lo}]}{dt} + \frac{d[\mathrm{NBD}_{li}]}{dt} = -k_-[\mathrm{NBD}_{lo}] - \frac{k_+}{1 + K_B[B]}([\mathrm{NBD}_T] - [\mathrm{NBD}_l])$$

$$[\mathrm{NBD}_w] = \frac{[\mathrm{NBD}_T] - [\mathrm{NBD}_l]}{1 + K_B[B]} \qquad (2)$$

The analytical solution for this set of equations is readily found for the case of fast or slow translocation resulting in eqs 3 or 4, respectively. If translocation occurs in the same time scale as interaction with the lipid bilayer, the differential equations shown in eq 2 must be solved numerically.

fast translocation : $k_f \gg k_-; k_+[\mathrm{LUV}]$

$$[\mathrm{NBD}_l](t) = \frac{[\mathrm{NBD}_T]2K_L[\mathrm{LUV}]}{1 + K_B[B] + 2K_L[LUV]}(1 - e^{-\beta t}); \quad K_L = \frac{k_+}{k_-}; \quad \beta = \frac{k_-}{2} + \frac{k_+[\mathrm{LUV}]}{1 + K_B[B]} \qquad (3)$$

slow translocation : $k_f \ll k_-; k_+[\mathrm{LUV}]$

$$[\mathrm{NBD}_l](t) = [\mathrm{NBD}_{lo}](t) = \frac{[\mathrm{NBD}_T]K_L[\mathrm{LUV}]}{1 + K_B[B] + K_L[\mathrm{LUV}]}(1 - e^{-\beta t}); \quad K_L = \frac{k_+}{k_-}; \quad \beta = k_- + \frac{k_+[LUV]}{1 + K_B[B]} \qquad (4)$$

In kinetic Scheme 2, and the corresponding rate equations, compartmentalization of the lipid phase was considered in the insertion step and the rate of insertion is given by the bimolecular insertion rate constant, k_+, multiplied by the concentration of lipid vesicles. This is in contrast with that considered in the previous section, Scheme 1, where the insertion rate was

Table 1. Kinetic and Thermodynamic Parameters for NBD-C_n Interaction with POPC LUVs and BSA, at 25 °C[a]

		translocation			desorption			insertion			
NBD-C_n	partition to POPC, K_P	k_f (s^{-1})	$\Delta H^{\ddagger 0}$ (kJ mol^{-1})	$T\Delta S^{\ddagger 0}$ (kJ mol^{-1})	k_- (s^{-1})	$\Delta H^{\ddagger 0}$ (kJ mol^{-1})	$T\Delta S^{\ddagger 0}$ (kJ mol^{-1})	k_+ (M^{-1} s^{-1})	$\Delta H^{\ddagger 0}$ (kJ mol^{-1})	$T\Delta S^{\ddagger 0}$ (kJ mol^{-1})	binding to BSA K_B (M^{-1})
$n = 8$	5.3×10^4	$3.8 \pm 0.2 \times 10^1$	69 ± 3	5 ± 3	$4.4 \pm 0.2 \times 10^1$	39 ± 3	−25 ± 3	$8.5 \pm 0.4 \times 10^{10}$	24 ± 3	13 ± 3	$5.2 \pm 0.3 \times 10^5$
$n = 10$	3.7×10^5	1.6 ± 0.3	93 ± 4	21 ± 4	5.1 ± 0.6	54 ± 5	−15 ± 5	$7.0 \pm 0.7 \times 10^{10}$	41 ± 4	30 ± 4	$5.8 \pm 1.3 \times 10^6$
$n = 12$	2.6×10^{6b}	$3.0 \pm 0.3 \times 10^{-1}$	80 ± 4	4 ± 4	$2.1 \pm 0.1 \times 10^{-1}$	64 ± 3	−13 ± 3	$2.0 \pm 0.1 \times 10^{10}$	51 ± 3	37 ± 3	$1.9 \pm 0.1 \times 10^{7c}$
$n = 14$	1.8×10^{7b}	$4.1 \pm 0.3 \times 10^{-1}$	62 ± 2	−13 ± 2	$1.2 \pm 0.2 \times 10^{-2}$	66 ± 6	−18 ± 6	$7.8 \pm 1.6 \times 10^9$	53 ± 6	37 ± 6	$2.4 \pm 0.7 \times 10^{7c}$
$n = 16$	1.3×10^{8b}	$1.7 \pm 0.1 \times 10^{-1}$	77 ± 2	0 ± 2	$7.6 \pm 1.3 \times 10^{-4}$	68 ± 6	−23 ± 6	$3.5 \pm 0.6 \times 10^9$	60 ± 3	42 ± 3	$5.5 \pm 1.9 \times 10^{7c}$

[a] The values shown represent the average and standard deviation of at least three independent experiments (usually five) for each amphiphile and temperature studied. [b] Values calculated from the linear best fit of $\ln(K_P)$ experimentally measured for NBD-C_4 to NBD-C_{10}.[1] [c] Calculated from the global best fit of eq 2 or 3 to the transfer of NBD-C_n between BSA and POPC LUVs.

Scheme 2. Kinetic Scheme for the Transfer of Amphiphile from BSA to POPC LUVs

$$\mathrm{NBD_w} \underset{k_-}{\overset{k_+[\mathrm{LUV}]}{\rightleftharpoons}} \mathrm{NBD_{\ell o}} \overset{k_f}{\longleftrightarrow} \mathrm{NBD_{\ell i}}$$
$$\Updownarrow K_B[\mathrm{B}]$$
$$\mathrm{NBD_B}$$

considered to be only dependent on the total surface of the lipid phase accessible to the amphiphile, S_l, and on the rate constant k_m with units of dm s^{-1}. The conversion between the two insertion rate constants is given by:

$$k_{in} = \frac{k_+}{\overline{S_{LUV}}/2} = \frac{k_+}{4\pi r^2 N_A} = \left.\frac{k_+}{1.9 \times 10^{12}}\right|_{100\ \mathrm{nm\ LUVs}} \quad (5)$$

In the rate expression for the insertion step used in this section the liposomes are considered as reactant species, and the values obtained for the bimolecular insertion rate constant may be compared with the rate constant predicted for a diffusion limited process ($k_{diff} = 4\pi r_{eff} D_{eff} N_A$). This comparison is very important because if the process is diffusion-limited, concentration gradients are generated, and therefore the topology of the lipid phase will influence the rate of amphiphile interaction.

For the case of the interaction of NBD-C_8 and NBD-C_{10} with POPC LUVs, the translocation occurred on the time scale of insertion/desorption, and therefore the results were analyzed via the numerical integration of eqs 2 with [B] = 0. The transfer for different concentrations of acceptor was followed, and the kinetic parameters were obtained from the global best fit to all experiments. Typical results obtained for NBD-C_8 are shown in Figures 4 and 5A, for NBD-C_{10}. It should be noted that for some concentrations of acceptor the transfer was not monoexponential and therefore all rate constants (k_f, k_+, and k_-) could be obtained from a single experiment; see insert in Figure 4B. We have opted to obtain the rate constants from the global best fit of the experiments for all acceptor concentrations to improve the accuracy in the parameters obtained.

For reasons given earlier, the kinetics of NBD-C_n ($n \geq 12$) were studied by first equilibrating the amphiphile with BSA and then transferring to POPC LUVs at different concentrations. The fluorescence increase that accompanied the transfer of the amphiphile from BSA to the LUVs was analyzed via the numerical integration of eqs 2 setting the value of the translocation rate constant initially at the value obtained in the previous section and allowing for some freedom around the average value. With this procedure it is possible to obtain accurately two of the remaining three unknown rate constants (k_+, k_-, and K_B). It is not possible to obtain both the equilibrium partition to the LUV and to the BSA, even with the global fit of transfer to different acceptor concentrations, and only the ratio between the two parameters may be obtained. Additionally, the partition to the lipid phase or the binding to BSA cannot be directly measured due to the low solubility of the amphiphiles in the aqueous media. We have solved this circular problem via the assumption of a linear dependence on the Gibbs free energy of partition to the lipid phase as a function of the length of the amphiphile alkyl chain (n). This is supported by the observation that this parameter changes linearly with n for NBD-C_4 to NBD-C_{10}[1] as well as for other homologous series of amphiphiles.[30−34] In some studies, for very hydrophobic amphiphiles, the increase observed in the partition coefficient as the hydrocarbon chain is

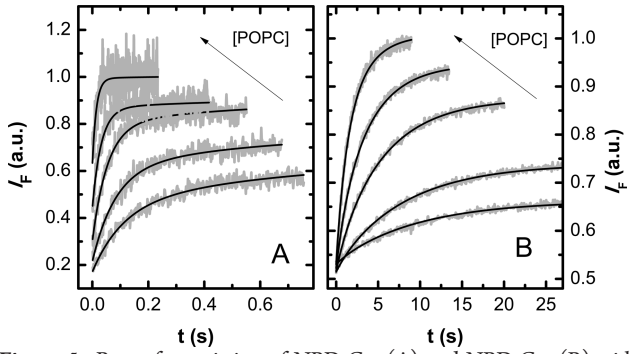

Figure 5. Rate of association of NBD-C_{10} (A) and NBD-C_{12} (B) with POPC LUVs at 25 °C. (A) Experimental results (gray line) obtained for [LUV] equal to 0.47, 0.93, 1.9, 3.7, and 9.3 × 10^{-10} M. The black lines are the global best fit of eq 2 with the rate constants $k_+ = 6.9 \times 10^{10}$ M^{-1} s^{-1}, $k_- = 5.1$ s^{-1}, and $k_f = 1.1$ s^{-1}. (B) Experimental results (gray line) obtained for [LUV] equal to 0.96, 1.9, 4.8, 9.7, and 19 × 10^{-10} M. The black lines are the global best fit of eq 2 with the rate constants $k_+ = 2.0 \times 10^{10}$ M^{-1} s^{-1}, $k_- = 2.1 \times 10^{-1}$ s^{-1}, $k_f = 2.6 \times 10^{-1}$ s^{-1}, and $K_B = 1.9 \times 10^7$ M^{-1}.

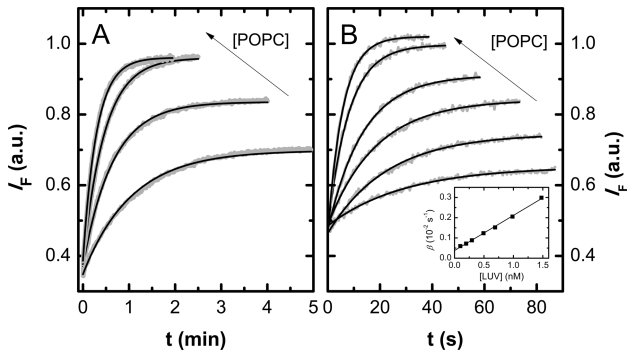

Figure 6. Rate of transfer of NBD-C_{14} (A) or NBD-C_{16} (B) from BSA at 50 μM to POPC LUVs at 25 °C. (A) Experimental results (gray line) obtained for [LUV] equal to 2.7, 5.5, 8.2, and 14 × 10^{-10} M. The black lines are the global best fit of eq 2 with the rate constants $k_+ = 7.9 \times 10^9$ M^{-1} s^{-1}, $k_- = 1.2 \times 10^{-2}$ s^{-1}, $k_f = 1.0 \times 10^{-1}$ s^{-1}, and $K_B = 2.2 \times 10^7$ M^{-1}. (B) Experimental results (gray line) obtained for [LUV] equal to 0.98, 2.0, 3.0, 4.9, 9.8, and 15 × 10^{-10} M. The black lines are the global best fit of eq 2 with the rate constants $k_+ = 3.6 \times 10^9$ M^{-1} s^{-1}, $k_- = 7.9 \times 10^{-4}$ s^{-1}, and $K_B = 4.3 \times 10^7$ M^{-1}. The insert shows the variation of the characteristic transfer rate constant (■) as a function of [LUV] and the best fit of eq 3 with the rate constants $k_+ = 3.5 \times 10^9$ M^{-1} s^{-1}, $k_- = 7.5 \times 10^{-4}$ s^{-1}, and $K_B = 4.0 \times 10^7$ M^{-1}.

lengthened is smaller than predicted from a linear dependence of ΔG°.[5,33,35] This curvature is only dependent on the overall hydrophobicity of the amphiphile and occurs at different hydrocarbon lengths for distinct homologous series. Therefore, it should reflect amphiphile aggregation in the aqueous phase (leading to a decrease in the apparent partition coefficient[36]) and is not in conflict with the prediction of a linear dependence of the Gibbs free energy of partition on the length of the hydrocarbon chain.[37]

The value of the equilibrium association of amphiphile with LUVs may be calculated from its partition coefficient using eq 6, where it is considered that the vesicle is formed by 10^5 lipid molecules with 0.795 dm^3 per mole of lipid[38] with the same volume in the outer and inner monolayers.

$$K_L = K_P \bar{V}_{LUV^{\circ}} = K_P \frac{\bar{V}_{LUV}}{2} = K_P \frac{7.95 \times 10^4}{2} \qquad (6)$$

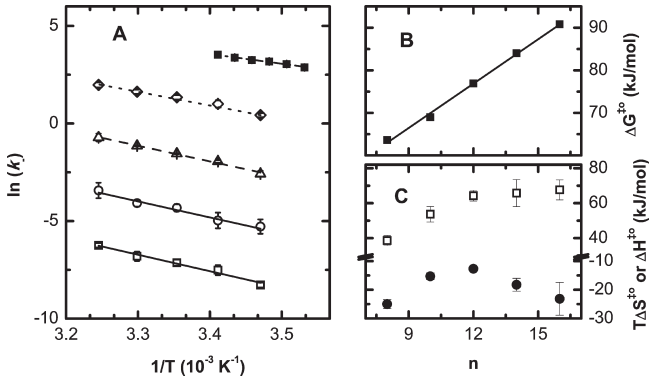

Figure 7. Kinetics and thermodynamics of NBD-C_n desorption from POPC bilayers. (A) Experimental results obtained for NBD-C_{16} (□, solid line), NBD-C_{14} (○, solid line), NBD-C_{12} (△, dashed line), NBD-C_{10} (◇, dotted line), and NBD-C_8 (■, dot−dashed line). The lines are the best fit of the absolute rate theory with the thermodynamic parameters at 25 °C shown in B for $\Delta G^{\ddagger o}$ (■) and C for $\Delta H^{\ddagger o}$ (□) and $T\Delta S^{\ddagger o}$ (●). The values shown are the average and standard deviation of at least three independent experiments for each amphiphile and temperature studied.

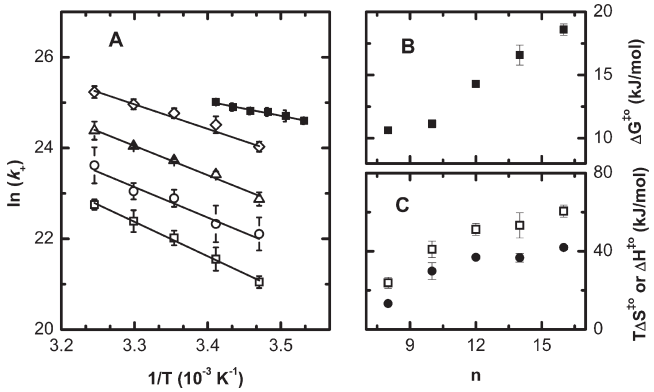

Figure 8. Kinetics and thermodynamics of NBD-C_n insertion into POPC LUVs. (A) Experimental results obtained for NBD-C_{16} (□), NBD-C_{14} (○), NBD-C_{12} (△), NBD-C_{10} (◇), and NBD-C_8 (■). The lines are the best fit of the absolute rate theory with the thermodynamic parameters at 25 °C shown in B for $\Delta G^{\ddagger o}$ (■) and in (C) for $\Delta H^{\ddagger o}$ (□) and $T\Delta S^{\ddagger o}$ (●). The values shown are the average and standard deviation of at least three independent experiments for each amphiphile and temperature studied.

For NBD-C_8 and NBD-C_{10} it is not necessary to impose a value for the equilibrium association with the LUVs because both insertion and desorption rate constants may be obtained from the best fit of eq 2. The value obtained for K_L is equal, within error, to that calculated from the measured partition coefficient via eq 6, giving confidence on the use of this approach for longer alkyl chain amphiphiles.

The transfer of NBD-C_{16} from BSA to POPC LUVs was very well-described by a monoexponential, Figure 6B. This behavior is due to the fact that translocation occurs much faster than insertion/desorption; therefore, the fast equilibrium approximation for translocation may be used, and the transfer is described by eq 3. Figure 6 shows the global best fit for the transfer of NBD-C_{14} (A) and NBD-C_{16} (B) to the different acceptor concentrations. The insert in Figure 6B shows the variation of the

characteristic rate constant for transfer (β, obtained from the best fit of a monoexponential to each experiment) with the acceptor concentration. Plots similar to the one shown in the insert of Figure 6B also permit obtaining the insertion and desorption rate constants.[39] The values obtained for the rate constants using both approaches were the same within error.

The association with the POPC LUVs was characterized at different temperatures and the variation of the thermodynamic parameters between the initial and the transition state were obtained using the absolute rate theory.[24] The results obtained are presented in Figures 7 and 8 and collectively given in Table 1. For the amphiphiles NBD-C_{10} to NBD-C_{16} the interaction with the POPC vesicles was studied between 15 and 45 °C. However, all processes were very fast for the case of NBD-C_8, and this amphiphile could only be characterized between 10 and 20 °C.

In Figure 7B, it can be seen that the Gibbs free energy for desorption from the POPC bilayer increases linearly with the length of the alkyl chain, reflecting the stronger interaction between the amphiphile hydrophobic portion and the membrane. The value obtained for $\Delta\Delta G^{\ddagger o}$, 3.4 ± 0.5 kJ mol^{-1}, is very similar to that obtained previously for homologous series of pyrene derivatized amphiphiles[40] and fatty acids[4] being slightly higher than the value found for double acyl chain phospholipids.[5,27] This increment per methylene group in the Gibbs free energy of desorption is larger than the modulus of the value found for partition to the lipid bilayer, $\Delta\Delta G^{o} = -2.4$ kJ mol^{-1}.[1] This indicates that the energy of the transition state in the desorption process, and its dependence on the length of the alkyl chain of the amphiphile, is larger than the energy of the amphiphile in the aqueous phase. Those results are in contradiction with recent studies by molecular dynamics simulations[41] where a monotonic increase in the Gibbs free energy as the amphiphile desorbs from the lipid bilayer into the aqueous phase is observed.

The decomposition in the enthalpic and entropic components shows two distinct regimes, the transition between them occurring at $n = 12$. For amphiphiles with a shorter alkyl chain, both the enthalpy and the entropy contribution to the Gibbs free energy of desorption increases strongly with n ($\Delta\Delta H^{\ddagger o}$ = 7.5 and 5.3 kJ mol^{-1} and $T\Delta\Delta S^{\ddagger o}$ = 4.8 and 1.3 kJ mol^{-1} for Δn = 8−10 and 10−12, respectively). In contrast, for amphiphiles with a longer alkyl chain the increment in the enthalpic contribution is very small ($\Delta\Delta H^{\ddagger o}$ = 0.8 and 0.9 kJ mol^{-1} for Δn = 12−14 and 14−16, respectively), and the entropy contribution decreases with the increase in the alkyl chain length ($T\Delta\Delta S^{\ddagger o}$ = −2.8 and −2.5 kJ mol^{-1} for Δn = 12−14 and 14−16, respectively). A smaller increment of the enthalpic contribution for longer chain amphiphiles has also been observed for phospholipid derivatives.[5] This result may be rationalized in concert with that obtained for the desorption of different homologous series of pyrene derivatives:[40] $\Delta\Delta H^{\ddagger o}$ = 3.5 kJ mol^{-1} for pyrene derivatized with an alkyl chain presenting a polar group at the extremity, and $\Delta\Delta H^{\ddagger o}$ = 8.4 kJ mol^{-1} for pyrene attached to an alkyl chain. In the case of alkyl pyrene the bulkier, and also highly polarizable, group of the aromatic moiety of the molecule should be located at the lipid bilayer interface, near the glycerol and first carbons of the lipid acyl chains, thereby reporting on the interactions that pyrene establishes with this region of the bilayer. In contrast, the strongly polar group at distal end of the alkyl chain (away from the aromatic group) of the other homologous series will anchor the amphiphile at the polar interface of the membrane and force the pyrene group to a position deeper in the lipid bilayer. For the latter group of amphiphiles, the bulky aromatic group is positioned in the highly disordered region of the bilayer center (below C_9), and the thermodynamics of the desorption process reports on the interactions established with this region of the bilayer. The behavior observed for the thermodynamic parameters of the desorption of the NBD-C_n homologous series indicates that amphiphiles with an alkyl chain shorter then $n = 12$ establish interactions with the more ordered region of the bilayer, while the alkyl chain of longer amphiphiles extends down to the center of the bilayer.

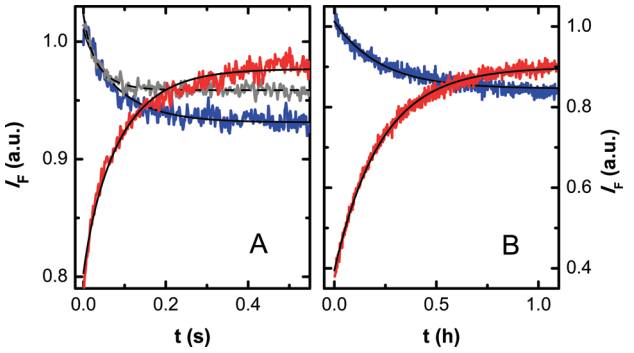

Figure 9. Exchange of NBD-C_n between BSA (or aqueous phase) and POPC LUVs. (A) Experimental results obtained for the transfer of NBD-C_8 from BSA to POPC (red solid line) and from POPC to BSA (blue solid line) for 10 μM BSA and 5.4 × 10^{-10} M POPC at 20 °C. The time variation of NBD-C_8 associated with POPC after dilution to half its initial concentration is also shown (gray dashed line). The black lines are the global best fit of eq 2 with the parameters: $k_+ = 4.6 \times 10^{10}$ M^{-1} s^{-1}, $k_- = 2.1 \times 10^{1}$ s^{-1}, $k_f = 2.0 \times 10^{1}$ s^{-1}, and $K_B = 5.2 \times 10^{5}$ M^{-1}. (B) Experimental results obtained for the transfer of NBD-C_{16} from BSA to POPC (red solid line) and from POPC to BSA (blue solid line) for 10 μM BSA and 1.1 × 10^{-10} M POPC LUVs, at 25 °C. The black lines are the global best fit of eq 2 with the parameters: $k_+ = 3.5 \times 10^{9}$ M^{-1} s^{-1}, $k_- = 7.6 \times 10^{-4}$ s^{-1}, and $K_B = 5.5 \times 10^{7}$ M^{-1}.

A complementary interpretation of the results may be given in terms of the behavior observed for the entropy variation, maximal at $n = 12$. This suggests that the entropy of the system (bilayer with inserted NBD-C_{12}) is the smallest along the homologous series with a better packing between the amphiphile and the lipids and a corresponding maximum in the attractive enthalpic contribution. Smaller or larger amphiphiles would constitute defects in the bilayer with relatively higher entropy in the inserted state (smaller increase when going to the transition state). This would explain the saturation of the enthalpic contribution due to the less tight interaction between the longer amphiphiles and the membrane. We have performed molecular dynamics simulations with the amphiphiles inserted in the POPC bilayer, and the results indicate that for alkyl chains longer than $n = 12$ there is a significant interdigitation of the amphiphile into the opposing monolayer and a higher conformational freedom of the alkyl chain at the center of the bilayer.[28] This larger conformational freedom of the inserted state generates a smaller entropy increase when going to the transition state.

The temperature dependence of the insertion rate constant and the variation of the thermodynamic parameters when going from the aqueous phase into the transition state are shown in Figure 8 for all amphiphiles in the NBD-C_n homologous series. The Arrhenius plots are linear for the longer amphiphiles but show clear deviations for the case of NBD-C_8 and NBD-C_{10}. This reflects the fact that for those amphiphiles the rate of insertion in

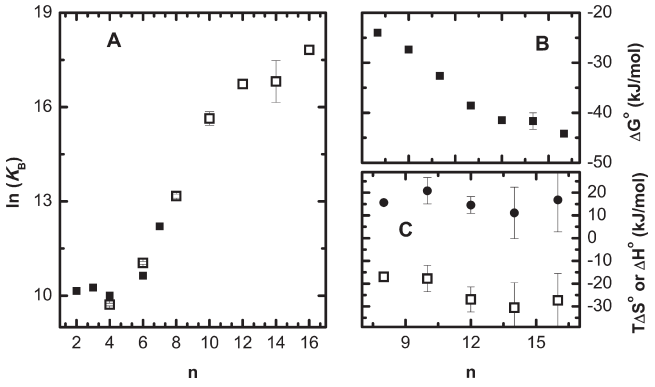

Figure 10. (A) Binding constant of NBD-C_n to BSA at 25 °C obtained in this work (□) and from literature (■).[44] The thermodynamic parameters obtained from the best fit of the van't Hoff equation are shown in B for ΔG^o (■) and C for ΔH^o (□) and $T\Delta S^o$ (●). The values shown are the average and standard deviation of at least three independent experiments for each amphiphile and temperature studied.

the lipid bilayer is close to that predicted for a diffusion-limited process and it may become controlled by diffusion at high temperatures. This behavior leads to the very small $\Delta G^{\ddagger o}$ observed for these two amphiphiles, Figure 8B. For NBD-C_{12} to NBC-C_{16}, $\Delta G^{\ddagger o}$ increases with the length of the alkyl chain, indicating a smaller probability of finding a cavity with the adequate dimensions in the bilayer during the time that the amphiphile, and the LUVs remain in close contact due to their diffusion-limited encounter.[42] An alternative interpretation for the increase in $\Delta G^{\ddagger o}$ with n could be the smaller solubility of the amphiphile in the ordered aqueous phase that solvates the lipid bilayer. This has been argued for the interaction of amphiphiles with cells due to the existence of the glycocalix and the corresponding unstirred layer[43] but should not be significant for the case of naked POPC LUVs.

In this work we show two types of independent experiments, the reaction of NBD-C_n with dithionite and NBD-C_n transfer between BSA and POPC LUVs, from which the translocation and the insertion/desorption rate constants have been, respectively, obtained. However, all kinetic parameters were required to analyze each of the experiments due to the multilamellarity in the LUVs (first section) and because translocation occurred in the same time scale as exchange (this section). The best fit shown is the final one after several iterations for convergence of the parameters obtained from both types of experiments.

Validation of the Kinetic Model. The experimental results shown in Figures 4 to 6 were obtained from the transfer of NBD-C_n from BSA (or from the aqueous solution for NBD-C_8 and NBD-C_{10}) to POPC LUVs and were very well-described by the kinetic model proposed. In this work the transfer at different concentrations of donor and/or acceptor was performed, and the parameters are obtained from the global best fit giving confidence as to their accuracy. Additionally, with the exception of NBD-C_8, two independent methods have been used to obtain the full set of parameters, one leading essentially to the translocation rate constant, while the other is mostly sensitive to the rate constants of insertion and desorption. Furthermore, the kinetic scheme should be validated by following the transfer of NBD-C_n in the reverse direction, from POPC to BSA or to the aqueous phase. This has been done, and the results obtained for the shorter and the longer amphiphiles in the homologous series are shown in Figure 9.

The same set of rate constants were used to describe the fluorescence decrease due to transfer of NBD-C_n from POPC to BSA (or to the aqueous phase) and the fluorescence increase due to transfer from BSA to POPC. The very good fit obtained is an important validation of the kinetic scheme used. In the model used it is assumed that the only effect of BSA in the transfer of amphiphile to the lipid bilayer is due to the decrease in the amphiphile concentration in the aqueous media. To validate this approach we have measured the rate of transfer of NBD-C_8 from the POPC bilayer to the aqueous phase and to BSA, Figure 9A. The results from both experiments were well-described by eq 2 using the same values for the rate constants (insertion, desorption, and translocation) and the measured binding constant between NBD-C_8 and BSA.[1] Those results indicate that transfer between BSA and the lipid bilayer occurs via the amphiphile in the aqueous media and that BSA may be used as a binding agent to allow the characterization of the interaction between the monomeric amphiphile and POPC lipid bilayers.

It should be noted that the fluorescence at equilibrium was not always the same for equal concentrations of binding agents and different transfer directions. The differences were not systematic, being interpreted as instrumental noise and uncertainty in the concentration of NBD-C_n.

Binding to BSA. From the rate of exchange between BSA and POPC vesicles, the equilibrium binding constant between the amphiphile and BSA is also obtained, and the results are shown in Figure 10. The first observation is the nonlinear dependency of $\ln(K_B)$, or ΔG^o, with n indicating an optimal amphiphile alkyl chain length of $n \approx 10$. The figure also includes the binding of additional NBD-C_n amphiphiles, with short alkyl chain lengths, obtained from the literature,[44] and the overall dependence of K_B with n suggests a significant interaction between the NBD group and the albumin that remains unchanged up to $n = 4$. For amphiphiles with an alkyl chain longer than 12 carbons, the increase in the binding affinity is smaller than predicted from the increase in the amphiphile hydrophobicity. This result was expected due to the relatively well-defined size of binding sites in proteins that can optimally accommodate a given ligand.

From the rate of amphiphile transfer between BSA and POPC LUVs, a lower limit for the rate of dissociation from BSA may be obtained. The characteristic rate constant for transfer was found to vary linearly with the concentration of acceptor, and this indicates that the dissociation from the donor is not the rate-limiting step. Considering the transfer rate constant obtained for the higher concentration of acceptor studied, one may conclude that the rate of dissociation from BSA is significantly larger than 2, 0.1, and 0.005 s^{-1} for NBD-C_{12}, NBD-C_{14}, and NBD-C_{16}, respectively.

CONCLUSIONS

The interaction of the amphiphiles in the NBD-C_n homologous series with POPC LUVs was completely characterized for $n = 8$ through $n = 16$, and all of the rate constants and their temperature dependence have been quantitatively obtained. This set of data allows the interpretation of the effects of the size of the amphiphile hydrophobic portion on the rate of each process being a valuable tool in the prediction of amphiphile bioavailability and pharmacokinetics in living systems.

It was found that the rate of translocation through POPC bilayers decreases as the hydrophobicity of the amphiphile is

increased for alkyl chains shorter than the thickness of the monolayer and that this parameter is not dependent on the length of the hydrophobic portion for longer chains. This behavior is easily interpreted if the transition state for translocation is considered to be the amphiphile in the center of the bilayer as the portion of the amphiphile already in this region of the bilayer will not contribute to the variations observed.

A transition between different regimes at $n = 12$ is also observed for the thermodynamic parameters of the desorption process. In this case the Gibbs free energy continues to increase with the length of the alkyl chain, because interactions between the amphiphile and the lipid bilayer that must be broken when going to the transition state are stronger, but the distinct characteristics of the inserted state may be recognized from the dependence of the thermodynamic parameters on the length of the alkyl chain. From the results obtained with this homologous series it is predicted that the portion of the amphiphile inserted in the center of the bilayer will not contribute significantly to the enthalpy variation upon formation of the transition state in the desorption process and that its entropy contribution will be unfavorable due to the large conformational freedom of the amphiphile in the inserted state. There is an enthalpy/entropy compensation and the Gibbs free energy for desorption varies linearly with the amphiphile hydrophobicity.

Another important conclusion that may be taken from this work is that insertion in the lipid bilayer is not diffusion-controlled although it does get very close to diffusion-controlled values for amphiphiles with a very short alkyl chain at high temperatures. This is in contrast with the behavior found for micelles,[45] and that has been assumed to apply to lipid bilayers as well although without any experimental support.[46] The difference observed for the two systems reflects the significantly larger area per lipid in the surface of the micelle as compared with that in a planar lipid bilayer. It is predicted that the rate of insertion should approach the diffusion limit as the curvature of the lipid assemblies is increased, as in the case of high density lipoproteins or SUVs. This has in fact been observed for the insertion and desorption of NBD-DMPE into lipoproteins of different curvature[42] and for the desorption of DMPC from SUVs and LUVs.[47] Recent results obtained by molecular dynamics simulations on lipid bilayers suggest the absence of any energy barrier in the insertion/desorption process of the interaction between amphiphiles and lipid bilayers,[41] a result that is in strong disagreement with those obtained in this work. We interpret this discrepancy as being a result of the simulation method used that allows the equilibration of the bilayer before the evaluation of the energetics of the amphiphile at different positions in the bilayer. In this way the contribution of the cavity left in the bilayer by the desorbing amphiphile is artificially removed from the energetics of the transition state.

From the kinetic parameters obtained in this work, the equilibrium distribution of the amphiphiles in the different compartments of biological systems may be calculated as well as their pharmacokinetics in the absence of specific transporters. The observation that insertion is not diffusion-limited introduces significant simplifications because concentration gradients will not be generated, and therefore the topology of the lipid phase will not influence the kinetics of the process. We are presently using these data in the calculation of the rate of passive permeation of these amphiphiles through tight endothelia such as the blood−brain barrier.

AUTHOR INFORMATION

Corresponding Author

*Address: Maria João Moreno, Departamento de Química da FCTUC, Largo D. Dinis, Rua Larga, 3004-535 Coimbra, Portugal. Phone: (+351) 239 854481. Fax: (+351) 239 827703. E-mail: mmoreno@ci.uc.pt.

ACKNOWLEDGMENT

This work was supported by research grants from the Portuguese Ministry for Science and Higher Education through FCT, via the PTDC program cofinanced by the European Union (Projects 64565 and 69072). R.M.S.C., F.G., and P.A.T.M. acknowledge FCT for their PhD fellowships with the reference SFRH/BD/45453/2008, SFRH/BD/40778/2007, and SFRH/BD/38951/2007, respectively.

REFERENCES

(1) Cardoso, R. M. S.; Filipe, H. A. L.; Gomes, F.; Moreira, N. D.; Vaz, W. L. C.; Moreno, M. J. *J. Phys. Chem. B* **2010**, *114*, 16337–16346.
(2) Massey, J. B.; Bick, D. H.; Pownall, H. J. *Biophys. J.* **1997**, *72*, 1732–1743.
(3) Thomas, R. M.; Baici, A.; Werder, M.; Schulthess, G.; Hauser, H. *Biochemistry* **2002**, *41*, 1591–1601.
(4) Zhang, F. L.; Kamp, F.; Hamilton, J. A. *Biochemistry* **1996**, *35*, 16055–16060.
(5) Nichols, J. W. *Biochemistry* **1985**, *24*, 6390–6398.
(6) Storch, J.; Kleinfeld, A. M. *Biochemistry* **1986**, *25*, 1717–1726.
(7) Pokorny, A.; Almeida, P. F. F.; Melo, E. C. C.; Vaz, W. L. C. *Biophys. J.* **2000**, *78*, 267–280.
(8) Kleinfeld, A. M.; Storch, J. *Biochemistry* **1993**, *32*, 2053–2061.
(9) Homan, R.; Pownall, H. J. *Biochim. Biophys. Acta* **1988**, *938*, 155–166.
(10) Moreno, M. J.; Estronca, L. M. B. B.; Vaz, W. L. C. *Biophys. J.* **2006**, *91*, 873–881.
(11) Sampaio, J. L.; Moreno, M. J.; Vaz, W. L. C. *Biophys. J.* **2005**, *88*, 4064–4071.
(12) Abreu, M. S. C.; Moreno, M. J.; Vaz, W. L. C. *Biophys. J.* **2004**, *87*, 353–365.
(13) Vaz, W. L. C.; Moreno, M. J.; Sampaio, J. L.; Abreu, M. S. C.; Vaz, C. T. A. *Biophys. Discuss.* **2004**, SP12A–SP12J.
(14) Andreas, M.; Peter, P. *ChemPhysChem* **2009**, *10*, 1405–1414.
(15) Fujikawa, M.; Ano, R.; Nakao, K.; Shimizu, R.; Akamatsu, M. *Bioorg. Med. Chem.* **2005**, *13*, 4721–4732.
(16) Sawada, G. A.; Barsuhn, C. L.; Lutzke, B. S.; Houghton, M. E.; Padbury, G. E.; Ho, N. F. H.; Raub, T. J. *J. Pharmacol. Exp. Ther.* **1999**, *288*, 1317–1326.
(17) Jing, P.; Rodgers, P. J.; Amemiya, S. *J. Am. Chem. Soc.* **2009**, *131*, 2290–2296.
(18) Abreu, M. S. C.; Estronca, L. M. B. B.; Moreno, M. J.; Vaz, W. L. C. *Biophys. J.* **2003**, *84*, 386–399.
(19) McIntyre, J. C.; Sleight, R. G. *Biochemistry* **1991**, *30*, 11819–11827.
(20) Peters, T. *All about Albumin. Biochemistry, Genetics, and Medical Applications*; Academic Press: New York, 1996.
(21) Bartlett, G. R. *J. Biol. Chem.* **1959**, *234*, 466–468.
(22) Moreno, M. J.; Bastos, M.; Velazquez-Campoy, A. *Anal. Biochem.* **2010**, *399*, 44–47.
(23) Smaby, J. M.; Momsen, M. M.; Brockman, H. L.; Brown, R. E. *Biophys. J.* **1997**, *73*, 1492–1505.
(24) Steinfeld, J. I.; Francisco, J. S.; Hase, W. L. *Chemical Kinetics and Dynamics*, 2nd ed.; Prentice-Hall: Upper Saddle River, NJ, 1999.
(25) Evans, M. G.; Polanyi, M. *Trans. Faraday Soc.* **1935**, *31*, 0875–0893.
(26) Eyring, H. *J. Chem. Phys.* **1935**, *3*, 107–115.

(27) Silvius, J. R.; Leventis, R. *Biochemistry* **1993**, *32*, 13318–13326.
(28) Filipe, H. A. L.; Moreno, M. J.; Loura, L. M. S. *J. Phys. Chem. B* **2011**DOI: 10.1021/203532c.
(29) Martins, P. A.; Gomes, F.; Vaz, W. L. C.; Moreno, M. J. *Biochim. Biophys. Acta* **2008**, *1778*, 1308–1315.
(30) Jain, M. K.; Wray, L. V. *Biochem. Pharmacol.* **1978**, *27*, 1294–1295.
(31) Peitzsch, R. M.; McLaughlin, S. *Biochemistry* **1993**, *32*, 10436–10443.
(32) Pool, C. T.; Thompson, T. E. *Biochemistry* **1998**, *37*, 10246–10255.
(33) Hoyrup, P.; Davidsen, J.; Jorgensen, K. *J. Phys. Chem. B* **2001**, *105*, 2649–2657.
(34) Heerklotz, H.; Epand, R. M. *Biophys. J.* **2001**, *80*, 271–279.
(35) Ho, J. K.; Duclos, R. I.; Hamilton, J. A. *J. Lipid Res.* **2002**, *43*, 1429–1439.
(36) Santos, A.; Rodrigues, A. M.; Sobral, A.; Monsanto, P. V.; Vaz, W. L. C.; Moreno, M. J. *Photochem. Photobiol.* **2009**, *85*, 1409–1417.
(37) Tanford, C. *The Hydrophobic Effect: Formation of Micelles and Biological Membranes*, 2nd ed.; Wiley: New York, 1980.
(38) Wiener, M. C.; White, S. H. *Biophys. J.* **1992**, *61*, 428–433.
(39) Estronca, L. M. B. B.; Moreno, M. J.; Vaz, W. L. C. *Biophys. J.* **2007**, *93*, 4244–4253.
(40) Pownall, H. J.; Hickson, D. L.; Smith, L. C. *J. Am. Chem. Soc.* **1983**, *105*, 2440–2445.
(41) Sapay, N.; Bennett, W. F. D.; Tieleman, D. P. *Soft Matter* **2009**, *5*, 3295–3302.
(42) Estronca, L. M. B. B.; Moreno, M. J.; Laranjinha, J. A. N.; Almeida, L. M.; Vaz, W. L. C. *Biophys. J.* **2005**, *88*, 557–565.
(43) Bojesen, I. N.; Hansen, H. S. *J. Lipid Res.* **2006**, *47*, 561–570.
(44) Matsushita, Y.; Takahashi, M.; Moriguchi, I. *Chem. Pharm. Bull.* **1986**, *34*, 333–339.
(45) Aniansson, E. A. G.; Wall, S. N.; Almgren, M.; Hoffmann, H.; Kielmann, I.; Ulbricht, W.; Zana, R.; Lang, J.; Tondre, C. *J. Phys. Chem.* **1976**, *80*, 905–922.
(46) Simard, J. R.; Kamp, F.; Hamilton, J. A. *Biophys. J.* **2008**, *94*, 4493–4503.
(47) Wimley, W. C.; Thompson, T. E. *Biochemistry* **1990**, *29*, 1296–1303.